ACS APPLIED MATERIALS & INTERFACES

Research Article

www.acsami.org

Influence of Gas Ambient on Charge Writing at the $LaAlO_3/SrTiO_3$ Heterointerface

Haeri Kim,[†] Seon Young Moon,[‡] Shin-Ik Kim,[‡,§] Seung-Hyub Baek,[‡,§] Ho Won Jang,[∥] and Dong-Wook Kim*[,†]

[†]Department of Physics, Ewha Womans University, Seoul 120-750, Republic of Korea

[‡]Electronic Materials Research Center, Korea Institute of Science and Technology (KIST), Seoul 136-791, Republic of Korea

[§]Department of Nanomaterials Science and Technology, University of Science and Technology, Daejeon, 305-333, Republic of Korea

[∥]Department of Materials Science and Engineering, Research Institute of Advanced Materials, Seoul National University, Seoul 151-742, Republic of Korea

Supporting Information

ABSTRACT: We investigated the influences of charge writing on the surface work function (W) and sheet resistance (R) of the $LaAlO_3/SrTiO_3$ (LAO/STO) heterointerface in several gas environments: H_2(2%)/N_2(98%), air, N_2, and O_2. The decrease in W and R due to charge writing was much larger in air ($\Delta W = -0.45$ eV and $\Delta R = -40$ kΩ/S) than in O_2 ($\Delta W = -0.21$ eV and $\Delta R = -19$ kΩ/S). The reduced R could be maintained more than 100 h in H_2/N_2. Such distinct behaviors were quantitatively discussed, based on the proposed charge-writing mechanisms. Such analyses showed how several processes, such as carrier transfer via surface adsorbates, surface redox, electronic state modification, and electrochemical surface reactions, contributed to charge writing in each gas.

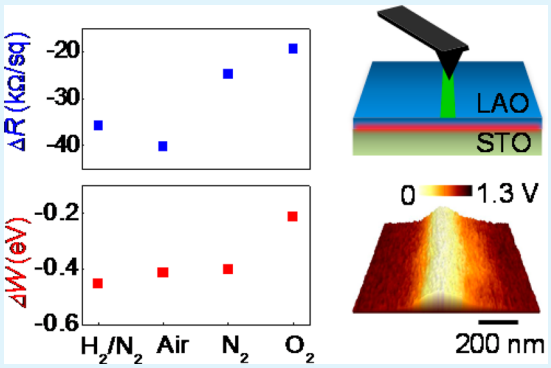

KEYWORDS: *$LaAlO_3/SrTiO_3$, carrier density, ambient effect, charge writing*

1. INTRODUCTION

High-mobility, two-dimensional (2D) conduction behaviors have been observed at the $LaAlO_3/SrTiO_3$ (LAO/STO) heterointerface.[1−24] Because both materials are wide-bandgap insulators, intensive experimental and theoretical research has been conducted to explain such extraordinary transport behavior.[1] The LAO/STO heterointerface has presented numerous unique physical properties, including a metal−insulator transition,[2−9] superconductivity,[10] magnetic ordering,[11−13] thermoelectricity,[14] electron correlation,[15] nonvolatile conductance control,[16] and a huge photoresponse.[17] The ongoing discovery of such phenomena has stimulated much research activity in relevant communities.

Among the variety of fascinating phenomena, modulation of local conductance using biased tip scanning (i.e., "charge writing") has received a great deal of attention for device applications as well as academic studies. It has been a long-standing obstacle to realize nanoscale patterning of metal oxides.[24−27] Etching damage caused by chemical and/or physical attack often severely deteriorates the physical properties of metal oxides. Thus, it is rather difficult to find in-depth studies on size effects and quantum transport in metal oxides. Recently, charge writing has been successfully used to fabricate oxide-based nanoelectronic devices.[2−9] Field-induced local desorption of surface adsorbates (the water-cycle mechanism) has been suggested as the origin of conductance modification.[7,18] Nanoscopic redox and the resulting increase in the carrier concentration offer another possibility.[19] Although experimental results led researchers to propose these scenarios, the mechanism has not been clarified to date.[6−9,18−21]

In this work, we investigated the influence of ambient gas and charge writing on the surface work function (W) and the sheet resistance (R) of the LAO/STO heterointerface in H_2/N_2, air, N_2, and O_2. The charge-writing experiments decreased both W and R of the samples in all ambient gas environments. The decrease in both W and R in air and H_2/N_2 was more notable than that in N_2 and O_2. The resistance retention characteristics in air and H_2/N_2 were also better than those in other gases. This indicated the importance of carrier transfer via charged surface adsorbates and oxygen vacancies during charge writing. Comparative investigations of the W and R reduction in the four gas ambients also revealed the contribution of additional processes, including electronic state modification and electrochemical reactions.

Received: May 29, 2014
Accepted: July 8, 2014
Published: July 8, 2014

2. EXPERIMENTAL SECTION

2.1. Sample Preparation. 4-nm thick LAO layers were deposited on TiO_2-terminated (001) STO substrates by pulsed laser deposition (PLD). A KrF excimer laser beam (wavelength: 248 nm; energy density: 1.5 J cm^{-2}; repetition rate: 2 Hz) was focused onto LAO single-crystal targets. The substrates were attached to a resistive heater and positioned 45−50 mm from the target. The LAO films were grown at a substrate temperature of 700 °C in an oxygen pressure of 1 mTorr. Detailed growth conditions and structural characterizations can be found in the authors' earlier publication.[16]

2.2. Transport Measurement. We fabricated a four-point measurement pattern and measured R of the 10 × 10 μm^2 active area, as shown in Figure 1a,b (see Supporting Information (SI) for details). The conducting region was confined only in the desired area by patterning an amorphous Al_2O_3 layer onto the STO substrates, as shown in the cross-sectional schematic diagram of Figure 1c.[16,24] An amorphous LAO (a-LAO) layer was formed on the Al_2O_3 layer and an epitaxial LAO (e-LAO) layer was formed on the STO substrate. Note that e-LAO growth occurred only on the STO substrate. The difference in the refractive indices and configuration of the top layers allowed the patterned area to be easily identified using an optical microscope, as shown in Figure 1b.

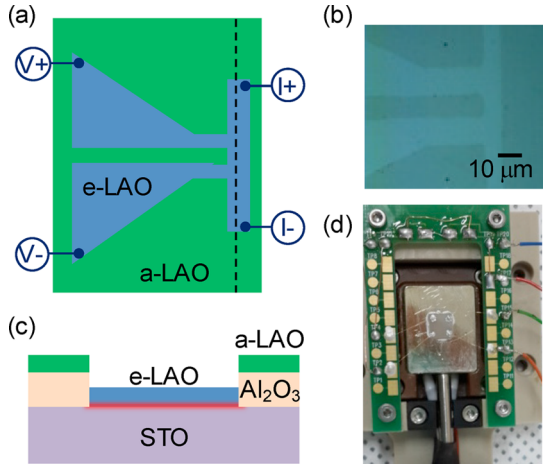

Figure 1. (a) Schematic diagrams of the $LaAlO_3/SrTiO_3$ (LAO/STO) sample for resistance measurements [green: amorphous-LAO (a-LAO) and blue: epitaxial-LAO (e-LAO)]. (b) Optical microscopy image of a patterned LAO/STO sample used in the four-point measurement. (c) Cross-sectional view of the dashed line in (a). (d) Optical microscopy image of the sample loaded on a heating stage for simultaneous Kelvin probe force microscopy (KPFM) and transport measurements.

2.3. Work Function Measurement. The surface work function (W) of the sample was measured by Kelvin probe force microscopy (KPFM) using an atomic force microscopy (AFM) system (XE-100, Park Systems Co.) with a glovebox. Four different ambient gases, H_2(2%)/N_2(98%), air (relative humidity: 20−30%), N_2, and O_2, were contained within a glovebox for the measurements. Transport and KPFM experiments were simultaneously performed in each of the ambient gas environments. The sample block was equipped with a heater and a printed circuit board (PCB) for electrical connection, as shown in Figure 1d. All of the measurements were conducted in the dark to exclude the possible influence of photocurrent (see SI Figure S1). Conductive Pt-coated Si cantilevers (NSG10/Pt, resonance frequency: ~240 kHz, NT-MDT) were used for charge writing and imaging of the LAO/STO sample surface. The charge-writing experiment was performed in contact mode by applying +10 V to the tip, which had a scan speed of 150 nm s^{-1}. The KPFM images were acquired by applying an alternating-current (AC) modulation voltage of 2 V and a frequency of 20 kHz to the tip, with a scan speed of 400 nm s^{-1}.

3. RESULTS AND DISCUSSION

3.1. Sheet Resistance and Work Function in H_2/N_2 and O_2. Figure 2a shows the R of the LAO/STO sample measured during repeated gas-exchange cycles in H_2/N_2 and O_2 (detailed experimental procedures can be found in SI Figure S2). The measured R in H_2/N_2 (42.7 ± 0.6 kΩ/S) was slightly smaller than that in O_2 (43.2 ± 0.4 kΩ/S). However, the variation of R during repeated measurements in each gas was large: R in H_2/N_2 was sometimes larger than that in O_2 (e.g., 1■ > 2●). Thus, the ambient dependence of R was not obvious. As shown in Figure 2b, all the W values measured in H_2/N_2 (4.49 ± 0.07 eV) were smaller than those in O_2 (4.75 ± 0.11 eV), indicating that W was more sensitive to the ambient than R.

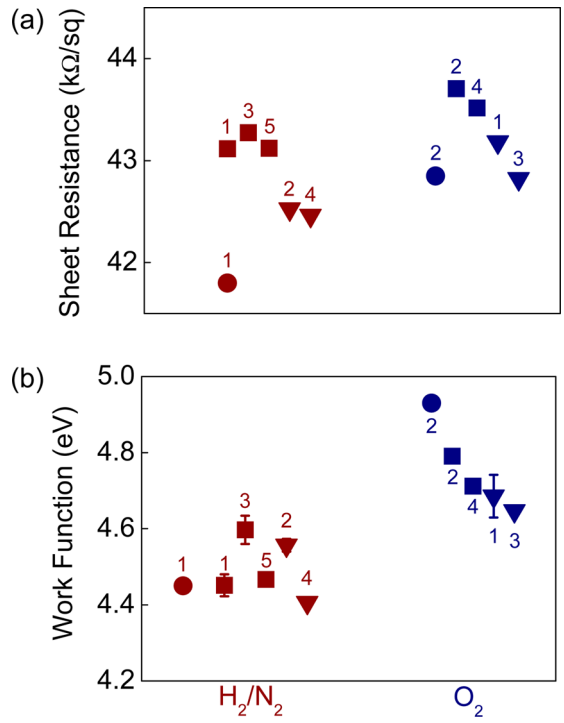

Figure 2. (a) Sheet resistance (R) and (b) work function (W) measured in H_2/N_2 and O_2. The error bars in the work function data indicate standard deviations of the data obtained from 2 × 2 μm^2 area scans. Symbols (●, ■, and ▼) and numbers represent the data obtained from three different sets of gas-exchange cycles and the measurement sequence in each set, respectively. Detailed experimental procedures can be found in SI Figure S2.

Recent theoretical work by Son et al. suggested that the adsorption of hydrogen generates surface hydrogen ion (H^+) adsorbates and induces electron donation to the LAO/STO interface.[21] The increase in the carrier concentration at the interface would reduce the sample resistance. The existence of charged adsorbates produces surface dipoles and lowers W, as illustrated in Figure 3a.[28] Such hydrogen adsorption/carrier donation scenario suggests that R and W in H_2/N_2 should be smaller than those in O_2.

Most of the complex oxides have predominantly ionic bonds and are prone to a variety of cationic and anionic defects, including vacancies, interstitials, and antisites. Defects should be present in the LAO thin film. The creation of a donor state at the surface via a redox reaction and subsequent electron transfer to the interface can increase interface carrier density.[19] At the same time, oxygen vacancies in LAO can decrease the

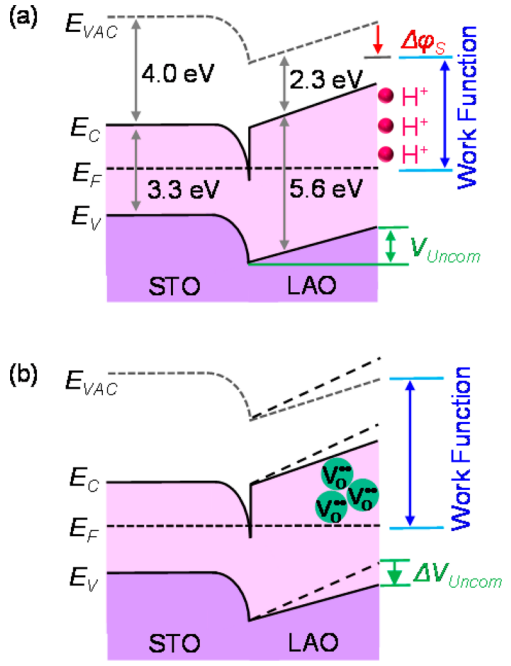

Figure 3. Band diagrams illustrating the effects of (a) adsorption and dissociation of H_2 to form H^+ surface adsorbates and (b) surface redox and lowering of the uncompensated potential, V_{Uncom}, due to oxygen vacancies ($V_O^{\bullet\bullet}$).

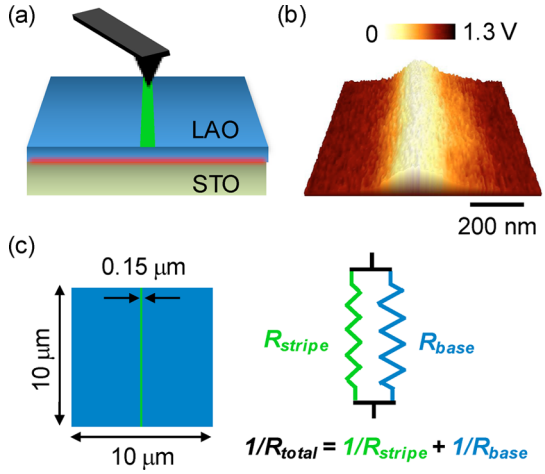

Figure 4. (a) Schematic diagram of the positively biased atomic force microscopy (AFM) tip used in the charge-writing process. (b) Map of contact potential difference (area: 1 × 1 μm^2) after charge writing in a H_2/N_2 atmosphere. (c) Schematic diagram of the scanned region ("stripe") and surrounding fresh region ("base").

uncompensated potential, V_{Uncom}, in the LAO film and W, as illustrated in Figure 3b. As described in SI Figure S2, the ambient-dependent measurements were repeated while exchanging gas ambient ("air → N_2 → H_2/N_2 → N_2 → O_2 → N_2 → H_2/N_2 → N_2 → O_2 → ⋯" or "air → N_2 → O_2 → N_2 → H_2/N_2 → N_2 → O_2 → N_2 → H_2/N_2 → ⋯"). Storage of the sample in O_2 would allow dissociation of O_2 molecules and the elimination of vacancies in LAO.[22] Thus, W and R in O_2 can be larger than those in H_2/N_2.

The hydrogen adsorption scenario allows us to quantitatively estimate the surface coverage, f, from W.[28] The potential drop by the dipole is given by $\Delta\varphi_s = e((f \times Ned)/\varepsilon)$ (N: number of unit cells per area; e: electron charge; d: dipole length; and ε: dielectric constant) (see Supporting Information for detailed calculations). d was assumed to be 2 Å (the H-metal bond length is known to be in the range of 1.75−2.06 Å).[29] $\Delta\varphi_s$ will vary with W, as schematically shown in Figure 3a. f of H^+ can be estimated to be 1.0 ± 0.3% from the difference of W in O_2 and H_2/N_2 because a negligible amount of H^+ adsorbates on the sample surface was expected in O_2. The resistance change at room temperature induced by the charge writing, ambient conditions, and growth conditions could be attributed to a change in the interface carrier density, σ, rather than the mobility.[23] Thus, f in H_2/N_2 can be also estimated to be 0.05 ± 0.05% from the measured R in H_2/N_2 and O_2, assuming carrier donation from each H atom (see SI for detailed calculations). These two values of f (1.0 ± 0.3 and 0.05 ± 0.05%) are largely different. Thus, the hydrogen adsorption and subsequent carrier donation scenario alone cannot well explain the ambient dependence of R and W.

3.2. Ambient Effects on Charge Writing. Figure 4a,b provide a schematic diagram of the charge-writing experiment and the W map of the LAO/STO sample, obtained after charge writing with an AFM tip, respectively. The biased tip was scanned over a local area, having a striped profile (stripe width: 150 nm; stripe length: 10 μm), on the active area for the measurement of R (area: 10 × 10 μm^2). The resistance drop was measured after writing. The sheet resistance of the area undergoing the charge writing, R_{stripe}, can be extracted from the total sheet resistance, R_{total}, after the charge writing and that of the fresh area, R_{base}, as shown in Figure 4c.

Figure 5 shows $\Delta R = R_{stripe} - R_{base}$ and $\Delta W = W_{stripe} - W_{base}$measured during the charge-writing experiments in all four gases for the charge-writing region ("stripe") and fresh region ("base"). The charge writing can modify the tip due to the application of relatively high voltage to the tip. To estimate the

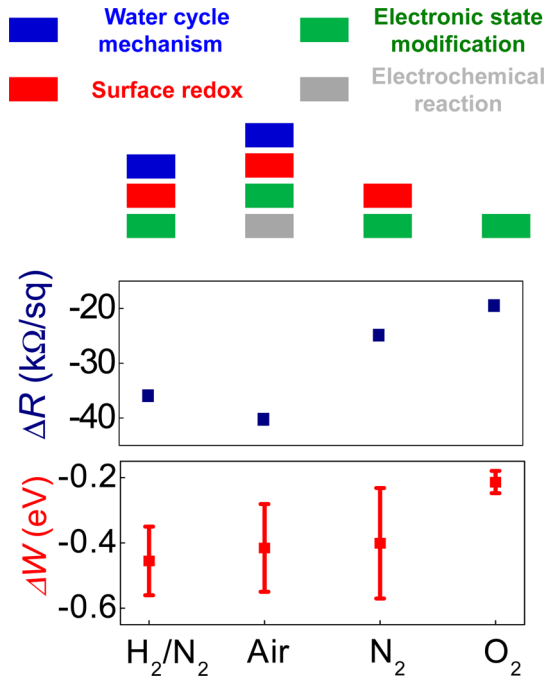

Figure 5. Differences in the sheet resistance ($\Delta R = R_{stripe} - R_{base}$) and work function ($\Delta W = W_{stripe} - W_{base}$) of the scanned and fresh areas. In each ambient, possible processes that cause the charge writing are listed above the plot.

dx.doi.org/10.1021/am503367f | ACS Appl. Mater. Interfaces 2014, 6, 14037−14042

W value reliably, careful calibration of the tip must be performed just before (or after) each measurement. Such repeated calibration is time-consuming. In this work, we measured the change of W in the charge-written area, ΔW, from the difference of W at two different areas ($W_{stripe} - W_{base}$). ΔW can clearly reveal the influence of the charge writing on W in each gas ambient without calibration. In air, $\Delta R = -40$ kΩ/S and $\Delta W = -0.45$ eV. These results were similar to those reported in the literature.[6−9] In O_2, $\Delta R = -19$ kΩ/S and $\Delta W = -0.21$ eV. The difference of R and W was the largest in air and the smallest in O_2.

Bi et al. proposed the water-cycle mechanism as the physical origin of charge writing.[7] In this process, water molecules adsorb on the surface and dissociate into OH^- and H^+ ions. The negatively charged OH^- ions can be removed by scanning of the positively biased tip. As a result, the surface coverage of H^+ can increase, and the remaining H^+ ions provide carriers to the interface, decreasing the sample resistance. On the basis of the water-cycle mechanism, the change in the H^+ surface coverage can be estimated from ΔW and ΔR, assuming negligible change in mobility.[23] From ΔR in air, the H^+ surface coverage was estimated to be 275%. In contrast, the coverage extracted from ΔW in air was only 1.6%. The significant difference in the H^+ surface coverage values suggested that the water cycle mechanism alone cannot explain both ΔR and ΔW.

Field-induced redox was considered as an alternative to explain charge writing. If the positively biased tip can remove oxygen ions from the LAO/STO sample, then oxygen vacancies are generated. Bristowe et al. suggested that oxygen vacancies can supply carriers to the interface and lower the uncompensated potential, V_{Uncom}.[19] According to such a scenario, $\Delta\sigma$ can be estimated by the following equation: $\Delta\sigma = -(\varepsilon_{LAO}/(e\ d_{LAO}))\Delta V_{Uncom}$ (ε_{LAO}: dielectric constant of LAO and d_{LAO}: LAO layer thickness].[23] In N_2, the environment has a negligible amount of water and H_2; thus, surface redox rather than the water-cycle mechanism may dominantly contribute to the charge-writing process. ΔV_{Uncom} will be equal to ΔW (see Figure 3b) because hydrogen adsorption is very unlikely to occur in N_2. Therefore, $\Delta\sigma$ can be estimated from ΔW. Alternatively, $\Delta\sigma$ can be determined by ΔR, according to the relationship, $\Delta(1/R) = \Delta\sigma \times e\mu$ (e: electron charge and μ: mobility). In N_2, $\Delta\sigma/\sigma$ estimated from ΔW is 0.14 ± 0.4. However, $\Delta\sigma/\sigma$ obtained from ΔR was 1.3 ± 0.0, almost ten times larger than that from ΔW. Therefore, field-induced redox (oxygen vacancy generation) alone could not explain the charge writing on the LAO/STO surface, even in hydrogen-free ambient.

Li and Yu reported systematic studies on the dissociation of water molecules in the LAO/STO system based on first-principles calculations.[20] They argued that the adsorption of water molecules had little effect on the electronic states of the LAO surface; however, the dissociation of water molecules could modify the electronic states of the LAO surface and the LAO/STO interface, leading to a metallic interface. For example, 1/4 surface coverage of water can raise the valence band maximum (VBM) of LAO by ∼0.2 eV. If such a process occurs, then W should increase and R should decrease. This is opposite to the trend predicted by the water-cycle mechanism and field-induced redox scenarios; for both of these cases, W and R decrease. Thus, the electronic state modification can help explain the aforementioned discrepancy of the $\Delta\sigma/\sigma$ values estimated from ΔR and ΔW ($\Delta\sigma/\sigma$ from $\Delta R > \Delta\sigma/\sigma$ from ΔW). Note that some of the water adsorbates could be removed by the baking process in our experiments (heating at 120 °C in N_2 gas), but chemisorbed water adsorbates are difficult to remove.[23]

Kumar et al. investigated the local electrochemical phenomena of charge writing on the LAO/STO surface, using electrochemical strain microscopy and KPFM.[9] They argued that the charge-writing mechanism should include somewhat complicated electrochemical components rather than simple screening by charged surface adsorbates. They also claimed that the electrochemical processes could be attributed to either surface charging due to electrochemical water-layer splitting or oxygen vacancy formation on or close to the material surface. As reported by many researchers, the large electric field produced by the biased tip can cause a variety of physical and electrochemical phenomena at the oxide surface in ambient air (mixture of various gases and water vapor).[28,30,31] For example, water adsorbates can form pillars of water between the tip and sample surface (capillary condensation), which results in contamination and unwanted electrochemical surface reactions. To avoid such complications, experiments can be performed under high-vacuum conditions.[30] Alternatively, measurements in controlled ambient are helpful to minimize the complicated effects.[28]

All the possible processes (i.e., the water-cycle mechanism, field-induced redox, electronic state modification, and electrochemical reactions) should be considered together to explain charge writing on the LAO/STO interface. The water-cycle mechanism (i.e., charge transfer via H adsorbates) should be important in H-containing environments (H_2/N_2 and air). The surface redox should also be considered, except for environments containing O_2. Redox reactions rarely occur in O_2, because the supply of O_2 from the ambient will continuously eliminate oxygen vacancies in LAO.[22] Electronic state modification via dissociation of water molecules can occur due to ambient water molecules and residual water adsorbates in air and all the dry gases. The electrochemical reaction will be more important in air than in other gases. The results in Figure 5 show the relative contribution of the listed mechanisms to charge writing. A large decrease in ΔR occurs in H_2/N_2 and air, indicating the importance of the water-cycle mechanism for reducing R during charge writing. The difference of ΔW in N_2 and O_2 is more notable than the difference of ΔR in the two gases. Thus, the contribution of the surface redox to lowering W is more important than that of the electronic state modification, as discussed above.

Figure 6 shows plots of ΔR as a function of time after the charge writing. The best retention is observed in H_2/N_2 among all the four gases used in this experiment, although ΔR is the largest in air. Also, the shortest retention time (∼2 days.) in O_2 is notable. As discussed above, the H adsorption and surface redox are important charge writing mechanisms. Such processes can readily occur in H_2/N_2, which can improve the retention of the resistance state. In contrast, the oxidation can return the sample resistance to the initial value.[22] As a result, the retention characteristics in the oxygen-containing gas (air and O_2) were worse than those in the nonoxidizing gas (H_2/N_2 and N_2,).

4. CONCLUSIONS

We investigated the effect of ambient gas on the charge writing at the LAO/STO heterointerface. The changes in R and W by the charge writing showed significant difference in the ambient gas, H_2(2%)/N_2(98%), air, N_2, and O_2. The retention characteristics of R also strongly depend on the gas environ-

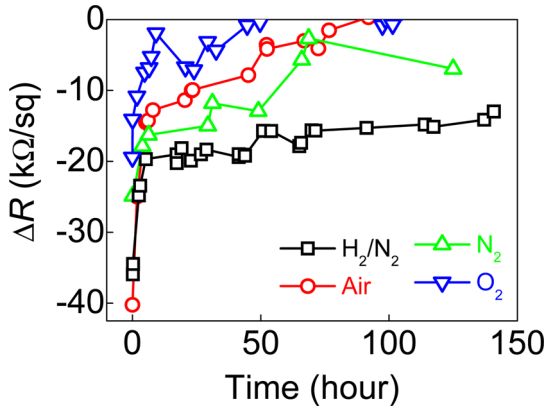

Figure 6. ΔR vs time after the charge writing in $H_2(2\%)/N_2(98\%)$, air, N_2, and O_2.

ment. The measured data were compared with those predicted from the proposed charge-writing mechanisms. A larger decrease of R occurred in H_2/N_2 and air, indicating that the water-cycle mechanism and redox played crucial roles in the reduction of R. Quantitative comparison of R and W in different gases also clearly indicated contribution of other mechanisms, such as the surface redox and the electronic state modification.

■ ASSOCIATED CONTENT

Ⓢ Supporting Information

Sheet resistance measurements, sheet resistance vs time plots, work flow of the ambient dependent measurements, and estimation of hydrogen surface coverage. This material is available free of charge via the Internet at http://pubs.acs.org.

■ AUTHOR INFORMATION

Corresponding Author

*Phone: +82 2 3277 6668; fax: +82 2 3277 2372; e-mail: dwkim@ewha.ac.kr.

Notes

The authors declare no competing financial interest.

■ ACKNOWLEDGMENTS

This work was supported by the Quantum Metamaterials Research Center (NRF-2008-0062236) and Basic Science Research Program (NRF-2013R1A1A2063744) through the National Research Foundation of Korea Grant, and the Korea Institute of Science and Technology (KIST) through 2E24881. H.W.J. acknowledges the Outstanding Young Researcher Program through the National Research Foundation of Korea.

■ REFERENCES

(1) Mannhart, J.; Blank, D. H. A.; Hwang, H. Y.; Millis, A. J.; Triscone, J.-M. Two-Dimensional Electron Gases at Oxide Interfaces. *MRS Bull.* **2008**, *33*, 1027−1034.

(2) Thiel, S.; Hammerl, G.; Schmehl, A.; Schneider, C. W.; Mannhart, J. Tunable Quasi-Two-Dimensional Electron Gases in Oxide Heterostructures. *Science* **2006**, *313*, 1942−1945.

(3) Cen, C.; Thiel, S.; Hammerl, G.; Schneider, C. W.; Andersen, K. E.; Hellberg, C. S.; Mannhart, J.; Levy, J. Nanoscale Control of an Interfacial Metal-Insulator Transition at Room Temperature. *Nat. Mater.* **2008**, *7*, 298−302.

(4) Cen, C.; Thiel, S.; Mannhart, J.; Levy, J. Oxide Nanoelectronics on Demand. *Science* **2009**, *323*, 1026−1030.

(5) Cheng, G.; Siles, P. F.; Bi, F.; Cen, C.; Bogorin, D. F.; Bark, C. W.; Folkman, C. M.; Park, J.-W.; Eom, C.-B.; Medeiros-Ribeiro, G.; Levy, J. Sketched Oxide Single-Electron Transistor. *Nat. Nanotechnol.* **2011**, *6*, 343−347.

(6) Xie, Y.; Bell, C.; Yajima, T.; Hikita, Y.; Hwang, H. Y. Charge Writing at the $LaAlO_3/SrTiO_3$ Surface. *Nano Lett.* **2010**, *10*, 2588−2591.

(7) Bi, F.; Bogorin, D. F.; Cen, C.; Bark, C. W.; Park, J.-W.; Eom, C.-B.; Levy, J. Water-Cycle" Mechanism for Writing and Erasing Nanostructures at the $LaAlO_3/SrTiO_3$ Interface. *Appl. Phys. Lett.* **2010**, *97*, 173110.

(8) Bark, C. W.; Sharma, P.; Wang, Y.; Baek, S. H.; Lee, S.; Ryu, S.; Folkman, C. M.; Paudel, T. R.; Kumar, A.; Kalinin, S. V.; Sokolov, A.; Tsymbal, E. Y.; Rzchowski, M. S.; Gruverman, A.; Eom, C. B. Switchable Induced Polarization in $LaAlO_3/SrTiO_3$ Heterostructures. *Nano Lett.* **2012**, *12*, 1765−1771.

(9) Kumar, A.; Arruda, T. M.; Kim, Y.; Ivanov, I. N.; Jesse, S.; Bark, C. W.; Bristowe, N. C.; Artacho, E.; Littlewood, P. B.; Eom, C.-B.; Kalinin, S. V. Probing Surface and Bulk Electrochemical Processes on the $LaAlO_3/SrTiO_3$ Interface. *ACS Nano* **2012**, *6*, 3841−3852.

(10) Reyren, N.; Thiel, S.; Caviglia, A. D.; Kourkoutis, L. F.; Hammerl, G.; Richter, C.; Schneider, C. W.; Kopp, T.; Rüetschi, A.-S.; Jaccard, D.; Gabay, M.; Muller, D. A.; Triscone, J.-M.; Mannhart, J. Superconducting Interfaces between Insulating Oxides. *Science* **2007**, *317*, 1196−1199.

(11) Brinkman, A.; Huijben, M.; Zalk, M.; van Huijben, J.; Zeitler, U.; Maan, J. C.; van der Wiel, W. G.; Rijnders, G.; Blank, D. H. A.; Hilgenkamp, H. Magnetic Effects at the Interface between Non-Magnetic Oxides. *Nat. Mater.* **2007**, *6*, 493−496.

(12) Bert, J. A.; Kalisky, B.; Bell, C.; Kim, M.; Hikita, Y.; Hwang, H. Y.; Moler, K. A. Direct Imaging of the Coexistence of Ferromagnetism and Superconductivity at the $LaAlO_3/SrTiO_3$ Interface. *Nat. Phys.* **2011**, *7*, 767−771.

(13) Li, L.; Richter, C.; Mannhart, J.; Ashoori, R. C. Coexistence of Magnetic Order and Two-Dimensional Superconductivity at $LaAlO_3/SrTiO_3$ Interfaces. *Nat. Phys.* **2011**, *7*, 762−766.

(14) Pallecchi, I.; Codda, M.; d'Agliano, E. G.; Marré, D.; Caviglia, A. D.; Reyren, N.; Gariglio, S.; Triscone, J.-M. Seebeck Effect in the Conducting $LaAlO_3/SrTiO_3$ Interface. *Phys. Rev. B* **2010**, *81*, 085414.

(15) Jang, H. W.; Felker, D. A.; Bark, C. W.; Wang, Y.; Niranjan, M. K.; Nelson, C. T.; Zhang, Y.; Su, D.; Folkman, C. M.; Baek, S. H.; Lee, S.; Janicka, K.; Zhu, Y.; Pan, X. Q.; Fong, D. D.; Tsymbal, E. Y.; Rzchowski, M. S.; Eom, C. B. Metallic and Insulating Oxide Interfaces Controlled by Electronic Correlations. *Science* **2011**, *331*, 886−889.

(16) Kim, S.-I.; Kim, D.-H.; Kim, Y.; Moon, S. Y.; Kang, M.-G.; Choi, J. K.; Jang, H. W.; Kim, S. K.; Choi, J.-W.; Yoon, S.-J.; Chang, H. J.; Kang, C.-Y.; Lee, S.; Hong, S.-H.; Kim, J.-S.; Baek, S.-H. Non-Volatile Control of 2DEG Conductivity at Oxide Interfaces. *Adv. Mater.* **2013**, *25*, 4612−4617.

(17) Chan, N. Y.; Zhao, M.; Wang, N.; Au, K.; Wang, J.; Chan, L. W. H.; Dai, J. Palladium Nanoparticle Enhanced Giant Photoresponse at $LaAlO_3/SrTiO_3$ Two-Dimensional Electron Gas Heterostructures. *ACS Nano* **2013**, *7*, 8673−8679.

(18) Li, F.; Liang, M.; Du, W.; Wang, M.; Feng, Y.; Hu, Z.; Zhang, L.; Wang, E. G. Writing Charge into the n-Type $LaAlO_3/SrTiO_3$ Interface: A Theoretical Study of the H_2O Kinetics on the Top AlO_2 Surface. *Appl. Phys. Lett.* **2012**, *101*, 251605.

(19) Bristowe, N. C.; Littlewood, P. B.; Artacho, E. Surface Defects and Conduction in Polar Oxide Heterostructures. *Phys. Rev. B* **2011**, *83*, 205405.

(20) Li, Y.; Yu, J. Modulation of Electron Carrier Density at the n-Type $LaAlO_3/SrTiO_3$ Interface by Water Adsorption. *J. Phys.: Condens. Matter* **2013**, *25*, 265004.

(21) Son, W.-J.; Cho, E.; Lee, J.; Han, S. Hydrogen Adsorption and Carrier Generation in $LaAlO_3$−$SrTiO_3$ Heterointerfaces: A First-Principles Study. *J. Phys.: Condens. Matter* **2010**, *22*, 315501.

(22) Trier, F.; Christensen, D. V.; Chen, Y. Z.; Smith, A.; Andersen, M. I.; Pryds, N. Degradation of the Interfacial Conductivity in

$LaAlO_3/SrTiO_3$ Heterostructures during Storage at Controlled Environments. *Solid State Ionics* **2013**, *230*, 12−15.
(23) Xie, Y.; Hikita, Y.; Bell, C.; Hwang, H. Y. Control of Electronic Conduction at an Oxide Heterointerface Using Surface Polar Adsorbates. *Nat. Commun.* **2011**, *2*, 494.
(24) Schneider, C. W.; Thiel, S.; Hammerl, G.; Richter, C.; Mannhart, J. Microlithography of Electron Gases Formed at Interfaces in Oxide Heterostructures. *Appl. Phys. Lett.* **2006**, *89*, 122101.
(25) Alexe, M.; Gruverman, A.; Harnagea, C.; Zakharov, N. D.; Pignolet, A.; Hesse, D.; Scott, J. F. Switching Properties of Self-Assembled Ferroelectric Memory Cells. *Appl. Phys. Lett.* **1999**, *75*, 1158−1160.
(26) Suzuki, N.; Tanaka, H.; Kawai, T. Epitaxial Transition Metal Oxide Nanostructures Fabricated by a Combination of AFM Lithography and Molybdenum Lift-Off. *Adv. Mater.* **2008**, *20*, 909−913.
(27) Hong, S.; Choi, T.; Jeon, J. H.; Kim, Y.; Lee, H.; Joo, H.-Y.; Hwang, I.; Kim, J.-S.; Kang, S.-O.; Kalinin, S. V.; Park, B. H. Large Resistive Switching in Ferroelectric $BiFeO_3$ Nano-Island Based Switchable Diodes. *Adv. Mater.* **2013**, *25*, 2339−2343.
(28) Kim, H.; Hong, S.; Kim, D.-W. Ambient Effects on Electric-Field-Induced Local Charge Modification of TiO_2. *Appl. Phys. Lett.* **2012**, *100*, 022901.
(29) Menetrey, M.; Markovits, A.; Minot, C. Reactivity of a Reduced Metal Oxide Surface: Hydrogen, Water and Carbon Monoxide Adsorption on Oxygen Defective Rutile $TiO_2(110)$. *Surf. Sci.* **2003**, *524*, 49−62.
(30) Lee, H.; Kim, H.; Van, T. N.; Kim, D.-W.; Park, J. Y. Nanoscale Resistive Switching Schottky Contacts on Self-Assembled Pt Nanodots on $SrTiO_3$. *ACS Appl. Mater. Interfaces* **2013**, *5*, 11668−11672.
(31) Kim, Y.; Morozovska, A. N.; Kumar, A.; Jesse, S.; Eliseev, E. A.; Alibart, F.; Strukov, D.; Kalinin, S. V. Ionically-Mediated Electromechanical Hysteresis in Transition Metal Oxides. *ACS Nano* **2012**, *6*, 7026−7033.

NOTE ADDED AFTER ASAP PUBLICATION

This paper was published on the Web on July 22, 2014, with minor graphical errors. The corrected version was reposted on July 29, 2014.